

Alginate-PLL Microencapsulation: Effect on the Differentiation of Embryonic Stem Cells Into Hepatocytes

Tim Maguire, Eric Novik, Rene Schloss, Martin Yarmush

Department of Biomedical Engineering, Rutgers University, 617 Bowser Road, Piscataway, New Jersey 08854; telephone: 732-445-3155; fax: 732-445-8184; e-mail: kma@soemail.rutgers.edu

Received 2 February 2005; accepted 13 September 2005

Published online 12 December 2005 in Wiley InterScience (www.interscience.wiley.com). DOI: 10.1002/bit.20748

Abstract: The emergence of hepatocyte based clinical and pharmaceutical technologies, has been limited by the absence of a stable hepatocyte cell source. Embryonic stem cells may represent a potential solution to this cell source limitation problem since they are highly proliferative, renewable, and pluripotent. Although many investigators have described techniques to effectively differentiate stem cells into a variety of mature cell lineages, their practicality is limited by: (1) low yields of fully differentiated cells, (2) absence of large scale processing considerations, and (3) ineffective downstream enrichment protocols. Thus, a differentiation platform that may be modified to induce and sustain differentiated cell function and scaled to increase differentiated cell yield would improve current stem cell differentiation strategies. Microencapsulation provides a vehicle for the discrete control of key cell culture parameters such as the diffusion of growth factors, metabolites, and wastes. In addition, both cell seeding density and bead composition may be manipulated. In order to assess the feasibility of directing stem cell differentiation via microenvironment regulation, we have developed a murine embryonic stem cell (ES) alginate poly-L-lysine microencapsulation hepatocyte differentiation system. Our results indicate that the alginate microenvironment maintains cell viability, is conducive to ES cell differentiation, and maintains differentiated cellular function. This system may ultimately assist in developing scalable stem cell differentiation strategies.

© 2005 Wiley Periodicals, Inc.

Keywords: alginate; encapsulation; hepatocytes; embryonic stem cells; differentiation

INTRODUCTION

The development of effective extracorporeal bioartificial liver devices (Demetriou et al., 2004; Hochleitner et al., 2005; Rahman et al., 2004; Shito et al., 2003; Tilles et al., 2002a,b; van de Kerkhove et al., 2004; Yarmush et al., 1992a,b; Zeilinger et al., 2004), in vitro systems for pharmaceutical toxicology studies (Xu et al., 2003), and biosensors for environmental toxins (Viravaidya et al., 2004), is currently limited by the absence of large numbers of

mature, functional hepatocytes. To address this cell source issue, research into alternate hepatocyte precursor populations has been conducted. One potential population that has been identified contains hepatic stem cells (hepatoblasts), which are not only capable of expressing differentiated hepatic function, but are also self-renewing (Dahlke et al., 2004; Newsome et al., 2004). A few hepatoblasts have been identified that can differentiate into mature hepatocytes, including bipotential precursors for hepatocytes and biliary cells (oval cells), and hematopoietic stem cells (Susick et al., 2001). Despite the fact that hepatoblasts potentially represent a renewable hepatocyte cell source, these cells are hard to isolate and exist in very low numbers (Tan et al., 2002). In addition, the efficacy of utilizing these precursor cells is questionable, since the long-term functional stability of hepatocytes obtained from these systems has yet to be assessed. As an alternative approach to hepatoblasts, many investigators have incorporated embryonic stem cell differentiation strategies into the generation of a renewable hepatocyte cell source using a variety of differentiation techniques (Chan et al., 2004; Hamazaki et al., 2001; Susick et al., 2001; Theise, 2003; Theise et al., 2000; Vessey and de la Hall, 2001). However, while hepatocyte function has been described, these strategies are limited in a number of ways, including the absence of large scale processing considerations, incomplete downstream enrichment techniques, and ineffective long-term functional maintenance. Thus, a culture environment that not only promotes hepatocyte function, but is also controllable, and scalable may alleviate the practical limitations of stem cell biotechnology.

Recently, studies have described the generation of scalable, controlled culture systems using alginate poly-L-lysine (PLL) encapsulation (Falasca et al., 2001; Rokstad et al., 2003; Selden et al., 1998). The benefits of alginate encapsulation system are numerous. First, alginate encapsulation beads can be depolymerized through the use of divalent cation chelators, facilitating rapid cell recovery for downstream analysis and application. Second, alginate encapsulation, through variations in the encapsulation process (i.e., alginate concentration, alginate composition, PLL

Correspondence to: M. Yarmush

Contract grant sponsors: NIH; NSF

Contract grant numbers: DK43371; DGE 0333196

concentration, bead diameter, and cell seeding density) can discretely control key culture parameters. Several investigators have described both the induction of adult stem cell differentiation, and increased function of mature hepatocytes following alginate encapsulation (Caterson et al., 2002; Kavalkovich et al., 2002; Khalil et al., 2001; Ma et al., 2003; Shakibaei and De Souza, 1997; Thompkins et al., 1988). In addition, alginate encapsulation has been used to maintain mature hepatocyte function within bioartificial livers (David et al., 2004; Dixit et al., 1992). Although these studies demonstrated that both adult hepatocyte cell function and adult mesenchymal stem cell differentiation could be induced and sustained within an alginate-PLL microenvironment, studies describing alginate encapsulation of embryonic stem cell populations to generate differentiated hepatocytes have been limited.

Despite the tremendous cell source potential of differentiated embryonic stem cells, most reported differentiation strategies are cumbersome, requiring embryoid body intermediates or specific growth factor supplementation. In addition these culture configurations often yield mixed cell populations (Hamazaki et al., 2001; Hu et al., 2003), even following the incorporation of embryoid bodies into alginate scaffolds (Gerecht-Nir et al., 2004). Thus, the present studies were initiated to investigate the feasibility of using alginate-PLL microencapsulation to direct the differentiation of single cell suspensions of embryonic stem cells into hepatocytes without the formation of embryoid bodies.

MATERIALS AND METHODS

Cell Culture

All cell cultures were incubated in a humidified 37°C, 5% CO₂ environment. The ES cell line D3 (ATCC, Manassas, VA) was maintained in an undifferentiated state in T-75 gelatin-coated flasks (Biocoat, BD-Biosciences, Bedford, MA) in Knockout Dulbecco's modified Eagles medium (Gibco, Grand Island, NY) containing 15% knockout serum (Gibco), 4 mM L-glutamine (Gibco), 100 U/mL penicillin (Gibco), 100 U/mL streptomycin (Gibco), 10 µg/mL gentamicin (Gibco), 1,000 U/mL ESGRO™ (Chemicon, Temecula, CA), 0.1 mM 2-mercaptoethanol (Sigma-Aldrich, St. Louis, MO). ESGRO™ contains leukemia inhibitory factor (LIF), which prevents embryonic stem cell differentiation. Every 2 days, media was aspirated and replaced with fresh media. Cultures were split and passaged every 6 days, following media aspiration, washing with 6 mL of phosphate buffered solution (PBS) (Gibco). Cells were detached following incubation with 3 mL of trypsin (Gibco) for 3 min, resulting in a single cell suspension, and subsequently the addition of 12 mL of Knockout DMEM. Cells were then replated in gelatin-coated T-75 flasks at a dilution of 1:15 and only passages 10 through 22 were used in the experiments. In order to induce differentiation, cells were suspended in Iscove's modified Dulbecco's medium (Gibco) containing 20% fetal bovine serum (Gibco), 4 mM L-glutamine (Gibco),

100 U/mL penicillin, 100 U/mL streptomycin (Gibco), 10 µg/mL gentamicin (Gibco). The Hepa 1-6 cell line (ATCC, Manassas, VA) was maintained in Dulbecco's modified Eagles medium (Gibco) containing 10% fetal bovine serum (Gibco), 100 U/mL penicillin (Gibco), 100 U/mL streptomycin (Gibco), and 4 mM L-glutamine (Gibco). Hepa1-6 cells were grown on tissue culture treated T-75 flasks (Falcon, BD Biosciences, San Jose, CA), and passages 10 through 22 were utilized for the experiments.

Alginate Poly-L-Lysine Encapsulation

An alginate solution was generated by dissolving 2.2 g of alginate (Sigma-Aldrich, MW: 100,000–200,000 g/mol, G-Content: 65%–70%) in 100 mL of Ca²⁺ free DMEM (Gibco), using a heated magnetic stir plate at a temperature of 45°C. The solution was then filtered using a 25-micron syringe filter (Fisher Brand, Pittsburg, PA). A confluent monolayer of adherent cells was removed following trypsin incubation, as described above, centrifuged for 10 min at 1,200 rpm, and resuspended in PBS. The cells were washed twice more with PBS (Gibco), resuspended in 2 mL of their respective media and both cell number and viability assessed using the method of trypan blue (Gibco) exclusion. To create the cell-alginate mixture a 1 mL aliquot of cell suspension with a seeding density of 5×10^7 cells/mL was added to 9 mL of a 2.2% (w/v) alginate solution to yield a final cell seeding density of 5×10^6 cells/mL and a final alginate concentration of 2.0% (w/v), (Fig. 1 Step A). This solution was transferred to a 10 mL syringe (BD Biosciences), which, in turn, was connected to a syringe pump (KD Scientific, Holliston, MA). Alginate beads were generated using an electrostatic bead generator (Nisco, Zürich, Switzerland) at a flow rate of 40 mL/h, and an applied voltage of 6.5 kV, resulting in beads with a diameter of 500 µm. The beads were extruded into a 200 mL bath of CaCl₂ (100 mM) (Sigma-Aldrich), containing 145 mM NaCl (Sigma-Aldrich), and 10 mM MOPS (Sigma-Aldrich) and were left to polymerize for 10 min at room temperature, (Fig. 1 Step B). Beads were transferred to a tissue culture treated T-25 flask (Falcon, BD Biosciences), following the polymerization step. The CaCl₂ solution was removed using a 5 mL pipette, and the beads were washed with 5 mL of HEPES (Gibco). The HEPES was removed and the beads were resuspended in 5 mL of poly-L-lysine (PLL) (Sigma-Aldrich, MW: 68,600 g/mol) (0.05% w/v) for 2 min. The PLL was then gently removed, replaced with HEPES to wash the beads and the beads were ultimately resuspended into 5 mL of cell culture media, (Fig. 1 Step C). Media was changed at days 4, 8, 11, 14, and 17 postencapsulation. In all experimental conditions, 7 day monolayer culture configurations of Hepa1-6 cells, were used as controls for viability, growth kinetics, and functional studies.

Assessment of Intracapsular Viability

Viability within beads was assessed with, a calcein (Molecular Probes, Eugene, OR), ethidium homodimer

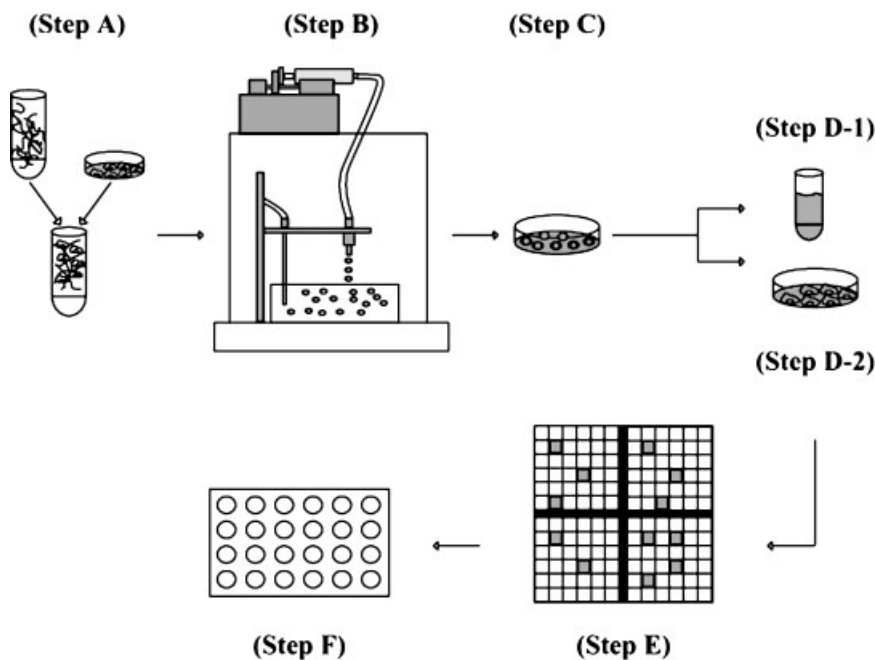


Figure 1. Schematic of encapsulation and analysis procedure. **Step A:** A cell suspension and alginate mixture is generated. **Step B:** Cells are encapsulated using an electrostatic bead generator, and a calcium chloride collecting solution. Beads are subsequently coated in PLL. **Step C:** Encapsulated cells are maintained 20 days in culture either in the presence or absence of LIF. **Step D-1:** The media is sampled for urea analysis. **Step D-2:** Beads are depolymerized, and cells recovered at days 8, 11, 14, 17, and 20 postencapsulation. **Step E:** Viability is assessed using a trypan blue exclusion assay. **Step F:** Recovered cells are transferred to a 24-well plate.

(Molecular Probes) stain, immediately following encapsulation. Calcein is only cleaved to form fluorescent products in live cells while ethidium homodimer is only incorporated into the nucleus of dead cells. Calcein and ethidium homodimer images were acquired using a Zeiss Axiovert LSM laser scanning confocal microscope (Germany) fitted with a 495 nm excitation filter and emission filters of 515 and 635 nm, respectively. Specifically, z-sections of 500 μm diameter beads were taken at 10 μm intervals, for a total depth of 250 μm . Three experiments incorporated an analysis of 15 beads per experiment. Digitized images were quantified using Olympus Microsuite. Viability was assessed for each cross-section of every bead.

Cell Recovery and Viability Assessment Following Depolymerization

Indirect immunofluorescent analysis and aggregate size calculations (see below) were performed one each of the analysis days following the release of cells from the beads, (Fig. 1 Step D-2). A minimum of 1,500 beads was analyzed per replicate per condition. Beads were washed with PBS, and 100 mM sodium citrate (Fisher Scientific), containing 10 mM MOPS (Sigma-Aldrich) and 27 mM NaCl (Sigma-Aldrich) was added for 30 min at 37°C to induce depolymerization. To determine recovery yield following depolymerization we encapsulated a known concentration of cells, and immediately depolymerized. Following centrifugation, we counted both the cell pellet as well as the supernatant (which contains bead particles but no intact

beads) using trypan blue exclusion (which does not stain the capsule), and after a mass balance, verified that we had approximately the same number of cells as in the starting population. This method demonstrated a 98% recovery of the encapsulated cell population. The released cells were centrifuged at 1,200 rpm for 10 min, the sodium citrate solution was aspirated, the cell pellet was washed with PBS (three times), and resuspended in cell specific media. The cells were then counted using the trypan blue method described above (Fig. 1 Step E).

Formation of Embryoid Body Control

Embryoid bodies (EB) were formed (day 0) and cultured for 2 days using the hanging drop method (1×10^3 ES cells per 30 μL drop). Hanging drops were transferred to suspension culture (day 2) in 100 mm Petri dishes (Falcon, BD Biosciences) and cultured for an additional 2 days. The EBs were then plated (day 4), one EB per well, in tissue culture treated six-well plates (Falcon, BD Biosciences). Media was changed at days 8, 11, and 14 postinduction of differentiation (day 0). Analysis of the EB system was limited to days 8, 11, 14, and 17, since the EBs overgrew the well plate following day 17.

In Situ Indirect Immunofluorescent Albumin Analysis

Cells recovered following depolymerization were transferred to a tissue culture treated 24-well plate (Falcon, BD

Biosciences), (Fig. 1 Step F). Specifically, the isolated cell population was diluted to 6×10^4 cells in 0.75 mL of media as was incubated for 1 h at 37°C to allow for cell attachment. The following procedure applies to both the EB system as well as cells recovered following depolymerization. The cells were then washed for 10 min in cold PBS and fixed in 4% paraformaldehyde (Sigma-Aldrich) in PBS for 15 min at room temperature. The cells were washed twice for 10 min in cold PBS and then twice for 10 min in cold saponine/PBS (SAP) membrane permeabilization buffer containing 1% bovine serum albumin (BSA) (Sigma-Aldrich), 0.5% saponine (Sigma-Aldrich), and 0.1% sodium azide (Sigma-Aldrich). The cells were subsequently incubated for 30 min at 4°C in a SAP solution containing rabbit anti-mouse albumin antibody (150 µg/mL) (MP Biomedicals, Irvine, CA), or normal rabbit serum (150 µg/mL) (MP Biomedicals) as an isotype control, washed twice for 10 min in cold SAP buffer, and then treated for 30 min at 4°C with the secondary antibody, FITC-conjugated donkey anti-rabbit, diluted 1:500 (Jackson Immuno Labs, Westgrove, PA). Cells were then washed once with cold SAP buffer and once with cold PBS. Fluorescent images were acquired using a computer-interfaced inverted Olympus IX70 microscope. Specimens were excited using a 515 nm filter. Fluorescent intensity values were determined for each cell using Olympus Microsuite. Experimental intensity values for each cell were calculated after subtracting the average intensity of the isotype control.

Urea Analysis

Media samples were collected directly from encapsulated cell cultures on days 8, 11, 14, 17, and 20 postencapsulation, (Fig. 1 Step D-1), and stored at -20°C for subsequent urea content analysis. Media samples were collected from the EB system on days 8, 11, 14, and 17 postinduction of differentiation, and stored at -20°C for subsequent urea content analysis. Urea synthesis was assayed using a commercially available kit (StanBio, Boerne, TX). A standard curve was generated by creating serial dilutions of a urea standard from 300 to 0 µg/mL. Absorbance readings were obtained using a Biorad (Hercules, CA) Model 680 plate reader with a 585 nm emission filter. Urea values were normalized to the cell number recorded on the day of media sample collection.

Intracapsular Aggregate Size Determination

Beads were sampled from the tissue culture treated T-25 flasks and transferred to 35 mm Mattek dishes (Mattek, Ashland, MA) immediately following encapsulation (day 0), and on the analysis days 8, 11, 14, 17, 20. Bright field images were acquired using a Zeiss Axiovert LSM laser scanning confocal microscope (Germany). Specifically, z-sections of 500 µm diameter beads were taken at 50 µm intervals, to avoid multiple quantification of the same aggregate, for a total depth of 250 µm. Images were quantified using Olympus Microsuite. In short, a color threshold was first applied in

order to distinguish cellular aggregates from the image background. The diameter of the aggregate was then determined using the mean diameter particle measurement.

Image Analysis Sample Size

The minimum sample size required for indirect immunofluorescent analysis of intracellular albumin was determined using Minitab Release 13, English Version (Minitab, Inc., State College, PA). The two-tailed two-sample *t*-test mode of the power algorithm was used with a population standard deviation of 5, to allow for large sample variation, a power value of 0.8, a significance level of 0.05, and a minimum difference (effect) of 3, for fine resolution between population means. The resultant minimum sample size that was calculated was 45 cells. To insure this sample size, 2 images (fields) were acquired per sample, and a minimum of 30 cells per image was quantified. For the aggregate size studies, the power algorithm was again implemented with a standard deviation of 0.1, a power value of 0.8, a significance level of 0.05 and a minimum difference of 0.25, thus allowing us to compare small differences in aggregate size. This yielded a minimum population size of 250 aggregates per experiment. This sample size was obtained by imaging 5 beads per experiment, with 5 cross sections per bead and a minimum of 10 aggregates per cross section.

Statistical Analysis

Each data point represents the mean, and the error bars represent the standard error of the mean. Statistical significance was determined using the Student's *t*-test for unpaired data. Differences were considered significant when the probability was ≤ 0.05 .

RESULTS

Assessment of Viability

An alginate-PLL murine embryonic stem cell encapsulation system was developed in order to investigate the feasibility of regulating hepatocyte differentiation within a controlled microenvironment and recovering differentiated cells from intracapsular culture. Our encapsulation system implements the electrostatic droplet approach, (Magyar et al., 2001), and resulted in a bead diameter of 500 µm at an applied voltage of 6.5 kV. The system is modified however, in that we maintained a solid bead core, thus maintaining the property of a single cell suspension. Initial experiments were designed to determine the cellular response to the alginate-PLL microencapsulation technique using both Hepa1-6 murine hepatoma cells and undifferentiated murine embryonic D3 cells. Immediately following encapsulation, beads were stained with calcein/ethidium homodimer, imaged, and the number of viable cells within the beads determined (Fig. 2). On average, the percent viability was reduced minimally from 98% to 95%, indicating that the encapsulation process

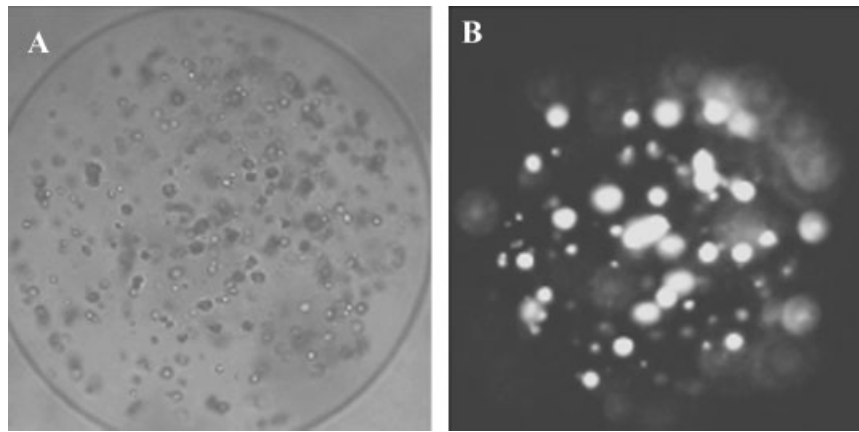


Figure 2. Assessment of intracapsular viability immediately following bead formation. Representative bright-field (A) and fluorescent images (B) of identical populations of encapsulated ES population observed at a magnification 20 \times . Fluorescent images were obtained through confocal cross sectioning of the beads following labeling with calcein/ethidium homodimer to evaluate cell viability.

caused little cell damage. We also assessed the effect of depolymerization and recovery on cell viability. As shown in Figure 3A, viability of encapsulated ES cells and Hepa1-6 cells was maintained at greater than 90% throughout the 20 day study. Growth kinetic studies (Fig. 3B), indicated that both encapsulated ES cells and Hepa1-6 cells, following an initial lag-phase, began to proliferate at approximately 14 days postencapsulation. In the case of ES cells, they ultimately reached a final density of 433 cells/bead, about 2.5 times greater than the initial density (168 cells/bead). Hepa1-6 cells reached a final density of 537 cells/bead, approximately 2.6 times higher than the initial density (206 cells/bead). These results indicate that neither encapsulation nor depolymerization significantly affected cell viability.

Mature Hepatocyte Function

Next, we evaluated cell function following alginate encapsulation. Two hepatocyte specific functions were assessed, urea secretion and intracellular albumin synthesis. Evaluation of intracellular albumin synthesis (as opposed to secreted albumin) allowed us to evaluate the function of individual cells with the population. As a measure of bulk population function, we used secreted urea as a marker for

mature hepatocyte function. Urea secretion was quantified using a commercially available kit and intracellular albumin synthesis was quantified using indirect immunofluorescence in conjunction with digital microscopy and image analysis. As seen in Figure 4A, while encapsulated Hepa1-6 cells exhibited significant levels of urea secretion during the 20 day culture period, undifferentiated ES cells maintained in LIF containing media, did not. In addition albumin synthesis was supported in the Hepa1-6 cell population whereas no significant albumin production was detected in the LIF supplemented ES cell population (Fig. 4B). Thus, encapsulation was able to support mature hepatocyte function in differentiated cells. Hepa1-6 function was comparable to values obtained in 7 day monolayer Hepa1-6 cultures, previous to plate overgrowth, for both urea secretion (Fig. 4C) and intracellular albumin production (Fig. 4B). However encapsulation did not induce differentiation in LIF supplemented ES cell populations.

Alginate Encapsulation and Embryonic Stem Cell Differentiation Culture

Subsequent studies were conducted to assess whether ES cells encapsulated in alginate-PLL beads would differentiate

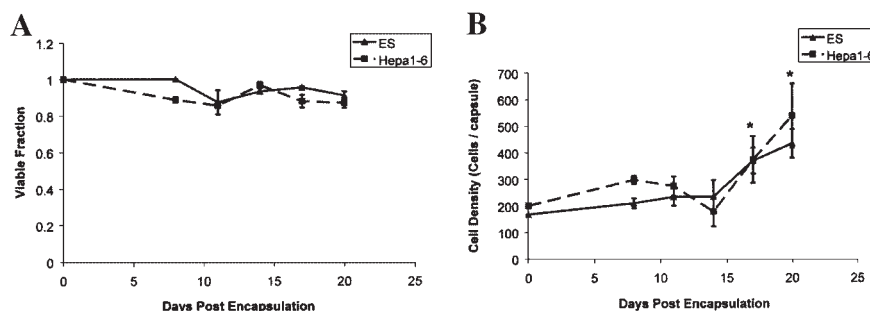


Figure 3. Comparison of viability (A) and growth kinetics (B) in encapsulated undifferentiated ES cells and Hepa1-6 cells. ES cells were encapsulated in 2.0% w/v alginate, at a cell seeding density of 5×10^6 cells/mL, and cultured in Knockout DMEM containing ESGROTM to prevent differentiation; Hepa 1-6 cells were encapsulated in 2.0% w/v alginate, at a cell seeding density of 5×10^6 cells/mL, and cultured in DMEM. Each data point represents the mean of a sample size of three experiments, and error bars represent standard error of the mean. Asterisks (*) designate a statistically significant difference ($P < 0.05$) for a time point as compared to day 0 for both ES cells and Hepa1-6 cells.

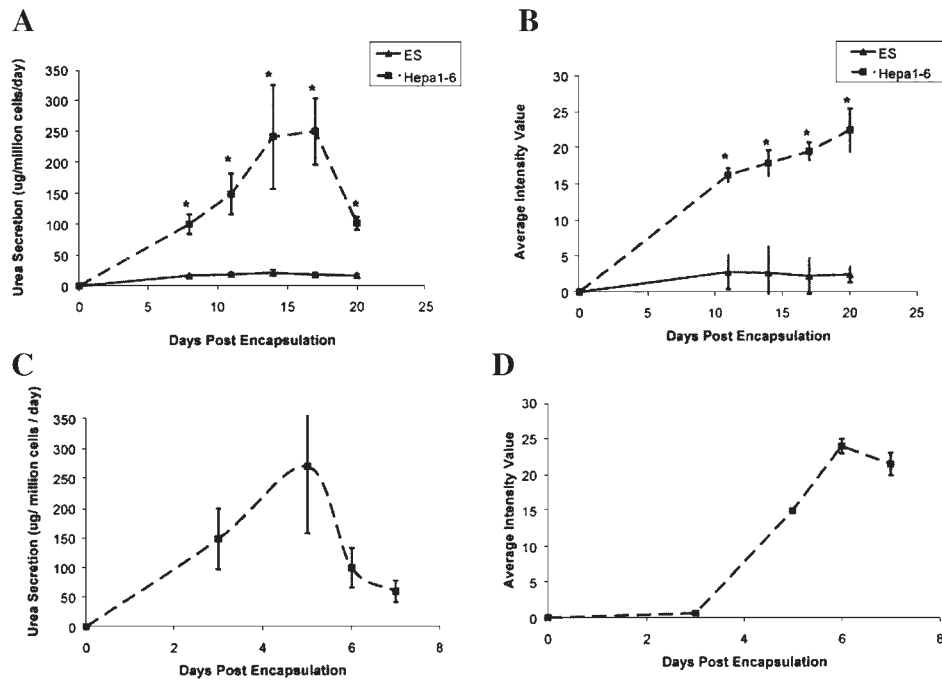


Figure 4. Urea secretion (A) and intracellular albumin levels (B) in encapsulated undifferentiated ES cells and Hepa1-6 cells. ES cells were encapsulated in 2.0% w/v alginate, at a cell seeding density of 5×10^6 cells/mL, and cultured in knockout DMEM containing ESGRO™ to prevent differentiation; Hepa 1-6 cells were encapsulated in 2.0% w/v alginate, at a cell seeding density of 5×10^6 cells/mL, and cultured in DMEM. **Panels C and D** depict monolayer Hepa1-6 urea secretion and intracellular albumin levels, respectively. Each data point represents the mean of a sample size of three experiments, and error bars represent standard error of the mean. Asterisks (*) designate a statistical difference between ES cells and Hepa1-6 cells ($P < 0.05$).

into hepatocytes or hepatocyte-like cells. Beads formed at a final cell concentration of 5×10^6 cells/mL (168 cells/bead) and an alginate concentration of 2.0% (w/v) were cultured in LIF-free media, and cell viability and growth kinetics assessed. The alginate concentration was selected as it was previously reported to re-establish encapsulated hepatocyte function (Falasca et al., 2001), and the initial cell seeding density was derived as the midpoint value from previous studies (Dvir-Ginzberg et al., 2003; Khalil et al., 2001). As shown in Figure 5A, the ES cell population retained greater than 95% viability and cells continued to divide during the first 10–15 days of culture. The maximum cell number was observed at day 14 postencapsulation (Fig. 5B), as the ES population reached a density of 291 cells/bead and remained constant thereafter.

Hepatocyte function was evaluated by measuring urea secretion and albumin synthesis. The results of urea secretion studies are summarized in Figure 6A and indicate that urea secretion was detected as early as day 8 following encapsulation, and maximum function ($458 \mu\text{g}/\text{million cells}/\text{day}$) was detected at day 20 postencapsulation. As indicated in Figure 6B, albumin synthesis followed the same kinetic trend. Albumin was detected by day 8 postencapsulation and reached a maximum level of expression at day 20. Thus alginate encapsulation could not only support ES cell viability and growth, but could also promote ES cell differentiation into hepatocyte lineage cells. Additionally, the encapsulation system yielded maximum functional values comparable to the EB differentiation system (urea secretion: $727 \mu\text{g}/\text{million cells}/\text{day}$; intracellular albumin

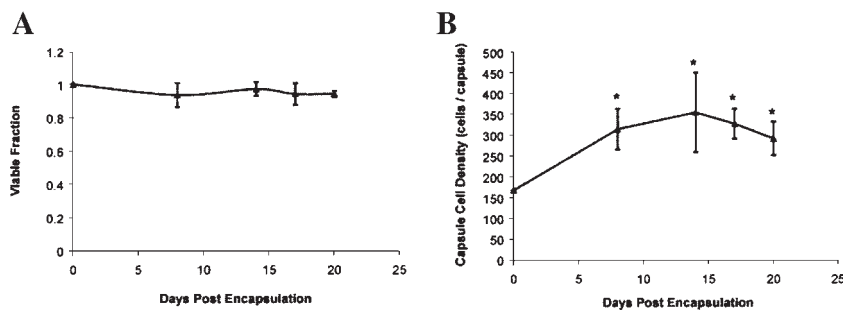


Figure 5. Viability (A) and growth kinetics (B) in an encapsulated ES cell population. ES cells were encapsulated in 2.0% w/v alginate, at a cell seeding density of 5×10^6 cells/mL, and cultured in Iscove's media. Each data point represents the mean of a sample size of 15 (five experiments done in triplicate), and error bars represent standard error of the mean. Asterisks (*) indicate a statistically significant difference ($P < 0.05$) from day 0.

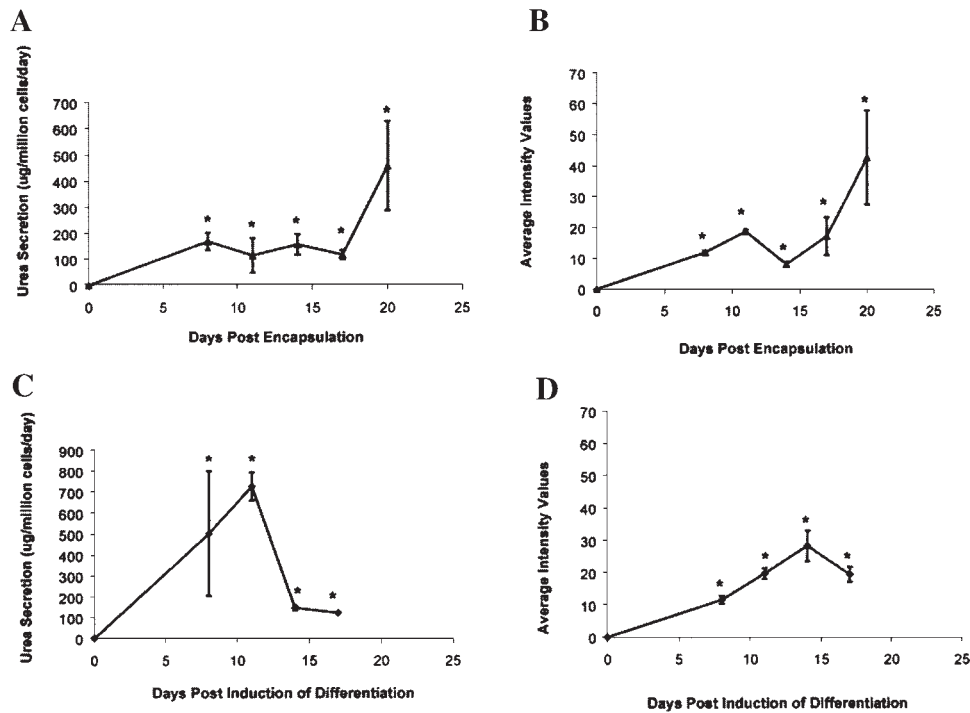


Figure 6. Urea secretion (A) and intracellular albumin levels (B) in encapsulated ES cells. ES cells encapsulated in 2.0% w/v alginate, at a cell seeding density of 5×10^6 cells/mL, and cultured in Iscove's media. Each data point represents the mean of a sample size of 15 (five experiments done in triplicate), and error bars represent standard error of the mean. Asterisks (*) indicate statistically significant differences ($P < 0.05$) from day 0. Panels C and D depict the embryoid body control for urea and intracellular albumin production, respectively.

production: 28.35) (Fig. 6C and D) and these values were sustained over time.

Cellular Aggregation During Differentiation

The next set of studies was designed to elucidate changes within the encapsulated cell population during differentiation. An initial qualitative evaluation of the encapsulated cell population indicated that a transition was made from a single cell suspension on day 0 to large cellular aggregates at day 20 (Fig. 7). Aggregate formation over time was then quantified using Microsuite to analyze bright field images obtained via confocal cross sectioning of the alginate-PLL beads. As indicated in Figure 8, average aggregate size increased linearly between days 11 and 20. Furthermore, while the initial functional peak (day 8) was not accompanied by large increases in aggregate size (day 11), maximum function as well as aggregate size were both detected at day 20 (Table I).

In order to further probe the relationship between aggregation and function, a subsequent set of studies was performed to assess the effect of initial cell seeding density on subsequent aggregation and hepatocyte function. In these studies four initial cell seeding densities (1×10^6 , 2×10^6 , 5×10^6 , 1×10^7 cells/mL) were established and aggregate size, urea secretion, percent albumin expressing differentiated cells and amount of albumin per cell were analyzed (Table II). As the cell seeding density was increased, the day 20 average aggregate size also increased, reaching a maximum (23.35 μm) at the highest cell seeding density

(1×10^7 cells/mL) examined. Hepatic function and yield however, appear to respond biphasically with respect to aggregate size, since both properties increased up to the 5×10^6 cells/mL cell seeding density, but then decreased at the highest cell seeding density (1×10^7 cells/mL) examined.

DISCUSSION

The adaptation of embryonic stem cell differentiation platforms into cell based clinical technologies has been impeded by inefficient differentiation strategies, which generally yield low numbers of differentiated cells within

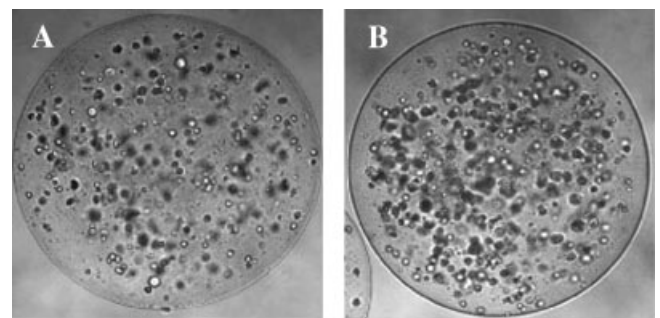


Figure 7. Qualitative comparison of aggregate formation during ES differentiation within bead environment. ES cells were encapsulated in 2.0% w/v alginate at a cell seeding density of 5×10^6 cells/mL, and cultured in Iscove's media. Representative images of encapsulated ES cells following the encapsulation process (A), and 20 days postencapsulation (B). Both images were taken at magnification $20\times$.

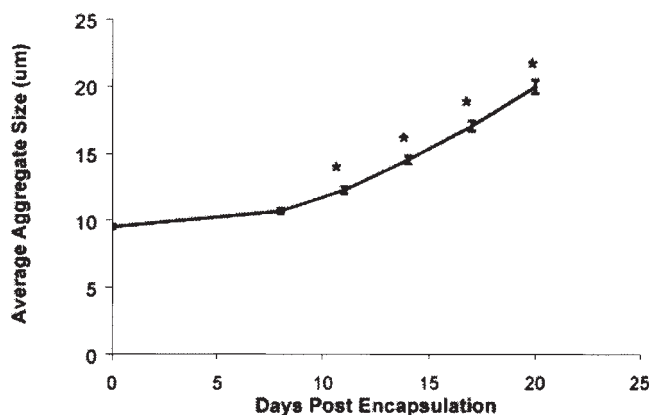


Figure 8. Kinetics of aggregate formation during ES differentiation. ES cells were encapsulated in 2.0% w/v alginate at a cell seeding density of 5×10^6 cells/mL, and cultured in Iscove's media. Each data point represents the mean of a sample size of three, and error bars represent standard error of the mean. Asterisks (*) indicate statistically significant differences ($P < 0.05$) from day 0.

mixed cell populations. In order to circumvent this problem, the current studies were designed to evaluate the feasibility of generating a scalable tissue culture environment using alginate encapsulation to promote embryonic stem cell differentiation into hepatocytes. Alginate-PLL encapsulation has been used extensively in the past (Sun et al., 1987, 1984), to promote adult stem cell differentiation (Steinert et al., 2003), to maintain mature hepatocyte function (David et al., 2004; Dixit et al., 1992), and to encapsulate embryoid bodies (EB), aggregates of ES cells traditionally used to induce differentiation (Magyar et al., 2001). In addition, alginate scaffolds have been utilized to promote EB differentiation (Gerecht-Nir et al., 2004). The current studies were designed to incorporate alginate-PLL encapsulation to control the differentiation of suspended murine ES cells into mature hepatocytes, thereby bypassing the cumbersome step of EB formation. Our data indicate that single cell suspensions of ES cells differentiated into hepatocyte lineage cells without significant loss in cell viability, and could be recovered from the beads following depolymerization for downstream analysis and application.

The encapsulation system was designed to limit the effect of oxygen transport on cell viability (Goosen, 1999). Beads were initially formed at a cell seeding density of 5×10^6

cells/mL and a 2.0% alginate concentration. An applied voltage of 6.5 kV was also used, leading to a bead size of 500 µm. After incorporating these parameters, we were able to demonstrate that alginate-PLL encapsulation provides a viable tissue culture environment for murine embryonic stem cells as well as Hepa1-6 murine hepatoma cells. Neither the encapsulation (Fig. 2) nor the depolymerization/recovery process significantly reduced cell viability. Furthermore, greater than 90% viability was maintained over the entire 20 day experimental period (Fig. 3A), indicating the feasibility of adapting alginate encapsulation into long term culture configurations. The initial characterization of our bead system included functional assessment of both encapsulated undifferentiated ES cells (cultured in the presence of LIF) and Hepa1-6 cells. Both encapsulated undifferentiated ES cells and Hepa1-6 cells demonstrated growth (Fig. 3B), following an initial lag-phase, which can be explained either by cell acclimation to the bead environment, (a phenomena that has been reported in other encapsulation systems (Rokstad et al., 2002)), or an initial balance between cell proliferation and cell death. Although ES cells continued to divide at the same rate as Hepa1-6 cells, ES cells cultured in LIF containing media, did not express mature hepatocyte function (Fig. 4A and B). This finding is noteworthy because it indicates the absence of transport limitations for LIF in the bead system. In addition, we demonstrated that the alginate-PLL beads can support hepatocyte function, since urea secretion and intracellular albumin production levels in encapsulated Hepa1-6 cells (Fig. 4A and B) were comparable to Hepa1-6 cells cultured in a monolayer configuration (Fig. 4C and D).

Our next objective was to determine whether the alginate-PLL beads could promote ES cell differentiation following LIF removal from the media. These experiments demonstrated that encapsulated ES cells increased both urea secretion and intracellular albumin production during the 20-day culture period, with maximum functional expression observed at day 20 (Fig. 6A and B). The observation of urea secretion in our system may be due to the uptake of glutamine and arginine, which are present in the culture media, (Chan et al., 2003). A noteworthy observation is the presence of a two-phase temporal functional response exhibited by the encapsulated ES population. Between days 8 and 14, postencapsulation, a peak in intracellular albumin production was observed at day 11, though at significantly lower levels

Table I. Assessment of aggregate size, urea synthesis, and intracellular albumin expression for an encapsulated ES cell population.

Days postencapsulation	Aggregate size (µm)	Urea secretion (µg/million cells/day)	Albumin average intensity value
0	9.56 ± 0.17	0.00 ± 0.00	0.00 ± 0.00
8	10.74 ± 0.19	169.15 ± 33.86	11.89 ± 0.60
11	12.30 ± 0.25	114.99 ± 66.26	18.68 ± 0.64
14	14.55 ± 0.30	157.40 ± 39.90	7.96 ± 0.71
17	17.05 ± 0.31	117.36 ± 18.60	17.14 ± 6.18
20	19.97 ± 0.48	457.93 ± 170.58	42.62 ± 15.19

Table II. Population characterization of encapsulated cell populations, at day 20 postencapsulation, subjected to changes in cell seeding density.

Cell seeding density (cells/mL) ^a	Aggregate size (μm) ^a	Urea secretion (μg/million cells/day) ^a	Percent of population stained positive for albumin ^a	Average fluorescence intensity for albumin positive cells ^a
1 × 10 ⁶	12.96 ± 0.23 ^b	259.37 ± 0.01	31 ± 2	8.19 ± 3.17
2 × 10 ⁶	14.89 ± 0.31 ^b	249.84 ± 0.02	35 ± 1	8.52 ± 4.62
5 × 10 ⁶	19.97 ± 0.48 ^b	457.93 ± 170.58 ^b	87 ± 3 ^b	42.62 ± 15.19 ^b
1 × 10 ⁷	23.35 ± 0.49 ^b	178.07 ± 17.76 ^b	72 ± 3 ^b	22.04 ± 3.80 ^b

^aEach data point represents the mean of a sample size of nine experiments (three experiments done in triplicate), and error bars represent standard error of the mean. All cell seeding densities were established simultaneously from the same starting ES cell population.

^bIndicate statistical significance from all other conditions ($P < 0.05$).

then the day 20 maximum. During the initial phases of differentiation, the ES cells may execute a preprogrammed path of differentiation until they become acclimated to the bead environment. Once acclimation exists, however, the bead microenvironment may play a key role in differentiation. A second key point is that the functional values we obtained for the encapsulation system were comparable to our gold standard (Novik et al., 2005), an EB culture formed using the hanging drop technique, allowed to spontaneously differentiate (Fig. 6C and D). However, function was maintained in the encapsulated system for a longer period of time. Furthermore, although differentiation efficiency was approximately the same in both differentiation systems, the encapsulation system is more advantageous since it is amenable to scale-up protocols, and uses a single cell suspension of undifferentiated ES cells (as determined in the aggregate studies for day 0 beads, Fig. 8A and B), thus bypassing the formation of an EB intermediate to induce differentiation, a process which makes cellular isolation of specific sub-populations difficult. These findings substantiate encapsulation as an alternative to traditional systems used for hepatocyte differentiation.

Many investigators have induced hepatocyte differentiation from ES cells following growth factor or extracellular matrix protein supplementation (Hamazaki et al., 2001; Suzuki et al., 2003). In these systems, the input parameter clearly plays a key role in hepatocyte differentiation. However, since in our encapsulation system, the cells were not induced to differentiate via hepatocyte specific mediator addition, the mechanism of differentiation is unclear. Other studies have described spontaneous ES differentiation into hepatocytes (Hu et al., 2003) via embryoid body culture. While embryoid bodies are known to generate three germ layers characteristic of embryo development, many paracrine responses may direct differentiation in those systems. However, in spite of the fact that embryoid bodies were neither included nor induced in our culture configuration, hepatocyte-like cells, or nonparenchymal cell that possibly arise within the cell population during differentiation, may produce auto-regulatory proteins, a phenomenon observed with hepatocytes in a sandwich configuration (Lee et al., 1993). In this case, the alginate may either induce or conserve this resource by limiting the diffusion of endogenously produced extracellular matrix or growth/differentiation inducing proteins. A second hypothesis is that alginate

entrapment may either promote cell–cell contact or decrease intercellular spacing. Both would be conducive to intercellular signaling mediated by direct contact or soluble mediators. Subsequent entrapment by alginate would further promote this interaction.

After demonstrating hepatocyte differentiation within the alginate-PLL system, we evaluated changes in population distribution within the alginate bead. An initial microscopic screening of the bead environment indicated that aggregate formation occurred during the 20-day differentiation period, Figure 7. Quantification of this aggregation process, Figure 8, demonstrated that aggregation initiation (around day 11 postencapsulation, Table I) lags behind the initial peak of cellular function (around day 8 postencapsulation, Table I). However the largest change in both function and aggregation were apparent between 17 and 20 days postencapsulation. Therefore cellular aggregation may be unnecessary during the initial stage. This may help to explain why aggregation in the context of EB formation may not be necessary initially in order to induce hepatic differentiation, but rather to augment the function of differentiated hepatocytes in the later stages of differentiation. In fact maximum *in vitro* hepatic function has been induced when mature hepatocytes are allowed to aggregate (Khalil et al., 2001; Semler et al., 2000; Takabatake et al., 1991).

To further investigate this hypothesis, we sought to modulate day 20 aggregate sizes through changes in the initial cell seeding density (Table II). In these experiments, we determined that, in general, increasing cell seeding density resulted in both increased aggregate size as well as functional enhancement. However, the functional response was biphasic, since the highest cell seeding density (1 × 10⁷ cells/mL) resulted in reduced hepatocyte function relative to the 5 × 10⁶ cells/mL seeding condition. This effect may result from the fact that at higher initial cell seeding densities, and ultimately larger aggregate sizes, the encapsulated aggregates may be regulated by nutrient limitations that possibly impede differentiated function. This effect has previously been observed in other high density culture configurations (Glicklis et al., 2004; Kavalkovich et al., 2002).

In summary, we have demonstrated that alginate-PLL encapsulation provides a scalable system to control embryonic stem cell differentiation into hepatocytes. While we have not evaluated the complete functional array characteristic of

mature hepatocytes, our results indicate that our encapsulated ES population displays at least two hepatocyte specific functions, urea and albumin synthesis. Future studies will be directed at expanding the analysis of hepatocyte function and to further probe the process of aggregate formation during the differentiation process. Through these ES encapsulation studies, we have established a promising approach to unravel key parameters involved in hepatocyte differentiation. In addition, this system may help to provide a renewable hepatocyte cell source needed for a variety of clinical and pharmaceutical applications.

These studies were supported by NIH DK43371, a grant from the NJ Commission on Higher Education, and The Graduate Fellowship Program on Integratively Engineered Biointerfaces at Rutgers, NSF DGE 0333196. The technical assistance of the following Rutgers BME students is also appreciated: Alex Davidovich, Marcy Hunter, Kristen Jenoriki, Tajneen Natasha, Biju Parekkadan, Jennifer Schloss, and Damini Shah.

References

- Caterson EJ, Li WJ, Nesti LJ, Albert T, Danielson K, Tuan RS. 2002. Polymer/alginate amalgam for cartilage-tissue engineering. *Ann N Y Acad Sci* 961:134–138.
- Chan C, Berthiaume F, Lee K, Yarmush ML. 2003. Metabolic flux analysis of cultured hepatocytes exposed to plasma. *Biotechnol Bioeng* 81(1):33–49.
- Chan C, Berthiaume F, Nath BD, Tilles AW, Toner M, Yarmush ML. 2004. Hepatic tissue engineering for adjunct and temporary liver support: Critical technologies. *Liver Transpl* 10(11):1331–1342.
- Dahlke MH, Popp FC, Larsen S, Schlitt HJ, Rasko JE. 2004. Stem cell therapy of the liver—fusion or fiction? *Liver Transpl* 10(4):471–479.
- David B, Dufresne M, Nagel MD, Legallais C. 2004. In vitro assessment of encapsulated C3A hepatocytes functions in a fluidized bed bioreactor. *Biotechnol Prog* 20(4):1204–1212.
- Demetriou AA, Brown RS, Jr., Busuttill RW, Fair J, McGuire BM, Rosenthal P, Am Esch JS II, Lerut J, Nyberg SL, Salizzoni M, et al. 2004. Prospective, randomized, multicenter, controlled trial of a bioartificial liver in treating acute liver failure. *Ann Surg* 239(5):660–667; discussion 667–670.
- Dixit V, Arthur M, Reinhardt R, Gitnick G. 1992. Improved function of microencapsulated hepatocytes in a hybrid bioartificial liver support system. *Artif Organs* 16(4):336–341.
- Dvir-Ginzberg M, Gamlieli-Bonshtein I, Agbaria R, Cohen S. 2003. Liver tissue engineering within alginate scaffolds: Effects of cell-seeding density on hepatocyte viability, morphology, and function. *Tissue Eng* 9(4):757–766.
- Falasca L, Miccheli A, Sartori E, Tomassini A, Conti Devirgiliis L. 2001. Hepatocytes entrapped in alginate gel beads and cultured in bioreactor: Rapid repolarization and reconstitution of adhesion areas. *Cells Tissues Organs* 168(3):126–136.
- Gerecht-Nir S, Cohen S, Ziskind A, Itskovitz-Eldor J. 2004. Three-dimensional porous alginate scaffolds provide a conducive environment for generation of well-vascularized embryoid bodies from human embryonic stem cells. *Biotechnol Bioeng* 88(3):313–320.
- Glicklis R, Merchuk JC, Cohen S. 2004. Modeling mass transfer in hepatocyte spheroids via cell viability, spheroid size, and hepatocellular functions. *Biotechnol Bioeng* 86(6):672–680.
- Goosen MF. 1999. Physico-chemical and mass transfer considerations in microencapsulation. *Ann N Y Acad Sci* 875:84–104.
- Hamazaki T, Iiboshi Y, Oka M, Papst PJ, Meacham AM, Zon LI, Terada N. 2001. Hepatic maturation in differentiating embryonic stem cells in vitro. *FEBS Lett* 497(1):15–19.
- Hochleitner B, Hengster P, Duo L, Bucher H, Klima G, Margreiter R. 2005. A novel bioartificial liver with culture of porcine hepatocyte aggregates under simulated microgravity. *Artif Organs* 29(1):58–66.
- Hu A, Cai J, Zheng Q, He X, Pan Y, Li L. 2003. Hepatic differentiation from embryonic stem cells in vitro. *Chin Med J (Engl)* 116(12):1893–1897.
- Kavalkovich KW, Boynton RE, Murphy JM, Barry F. 2002. Chondrogenic differentiation of human mesenchymal stem cells within an alginate layer culture system. *In Vitro Cell Dev Biol Anim* 38(8):457–466.
- Khalil M, Shariat-Panahi A, Tootle R, Ryder T, McCloskey P, Roberts E, Hodgson H, Selden C. 2001. Human hepatocyte cell lines proliferating as cohesive spheroid colonies in alginate markedly upregulate both synthetic and detoxificatory liver function. *J Hepatol* 34(1):68–77.
- Lee J, Morgan JR, Tompkins RG, Yarmush ML. 1993. Proline-mediated enhancement of hepatocyte function in a collagen gel sandwich culture configuration. *FASEB J* 7(6):586–591.
- Ma HL, Hung SC, Lin SY, Chen YL, Lo WH. 2003. Chondrogenesis of human mesenchymal stem cells encapsulated in alginate beads. *J Biomed Mater Res* 64A(2):273–281.
- Magyar JP, Nemir M, Ehler E, Suter N, Perriard JC, Eppenberger HM. 2001. Mass production of embryoid bodies in microbeads. *Ann N Y Acad Sci* 944:135–143.
- Newsome PN, Hussain MA, Theise ND. 2004. Hepatic oval cells: Helping redefine a paradigm in stem cell biology. *Curr Top Dev Biol* 61:1–28.
- Novik E, Maguire TJ, Orlova K, Schloss R, Yarmush ML. 2005. Embryoid body mediated differentiation of mouse embryonic stem cells along a hepatocyte lineage: Insights from gene expression profiles. *Tissue Eng* (in press).
- Rahman TM, Selden C, Khalil M, Diakanov I, Hodgson HJ. 2004. Alginate-encapsulated human hepatoblastoma cells in an extracorporeal perfusion system improve some systemic parameters of liver failure in a xenogeneic model. *Artif Organs* 28(5):476–482.
- Rokstad AM, Holtan S, Strand B, Steinkjer B, Ryan L, Kulseng B, Skjak-Braek G, Espevik T. 2002. Microencapsulation of cells producing therapeutic proteins: Optimizing cell growth and secretion. *Cell Transplant* 11(4):313–324.
- Rokstad AM, Strand B, Rian K, Steinkjer B, Kulseng B, Skjak-Braek G, Espevik T. 2003. Evaluation of different types of alginate microcapsules as bioreactors for producing endostatin. *Cell Transplant* 12(4):351–364.
- Selden C, Roberts E, Stamp G, Parker K, Winlove P, Ryder T, Platt H, Hodgson H. 1998. Comparison of three solid phase supports for promoting three-dimensional growth and function of human liver cell lines. *Artif Organs* 22(4):308–319.
- Semler EJ, Ranucci CS, Moghe PV. 2000. Mechanochemical manipulation of hepatocyte aggregation can selectively induce or repress liver-specific function. *Biotechnol Bioeng* 69(4):359–369.
- Shakibaei M, De Souza P. 1997. Differentiation of mesenchymal limb bud cells to chondrocytes in alginate beads. *Cell Biol Int* 21(2):75–86.
- Shito M, Tilles AW, Tompkins RG, Yarmush ML, Toner M. 2003. Efficacy of an extracorporeal flat-plate bioartificial liver in treating fulminant hepatic failure. *J Surg Res* 111(1):53–62.
- Steinert A, Weber M, Dimmler A, Julius C, Schutze N, Noth U, Cramer H, Eulert J, Zimmermann U, Hendrich C. 2003. Chondrogenic differentiation of mesenchymal progenitor cells encapsulated in ultrahigh-viscosity alginate. *J Orthop Res* 21(6):1090–1097.
- Sun AM, O'Shea GM, Goosen MF. 1984. Injectable microencapsulated islet cells as a bioartificial pancreas. *Appl Biochem Biotechnol* 10:87–99.
- Sun AM, Cai Z, Shi Z, Ma F, O'Shea GM. 1987. Microencapsulated hepatocytes: An in vitro and in vivo study. *Biomater Artif Cells Artif Organs* 15(2):483–496.
- Susick R, Moss N, Kubota H, Lecluyse E, Hamilton G, Luntz T, Ludlow J, Fair J, Gerber D, Bergstrand K, et al. 2001. Hepatic progenitors and strategies for liver cell therapies. *Ann N Y Acad Sci* 944:398–419.

- Suzuki A, Iwama A, Miyashita H, Nakauchi H, Taniguchi H. 2003. Role for growth factors and extracellular matrix in controlling differentiation of prospectively isolated hepatic stem cells. *Development* 130(11):2513–2524.
- Takabatake H, Koide N, Tsuji T. 1991. Encapsulated multicellular spheroids of rat hepatocytes produce albumin and urea in a spouted bed circulating culture system. *Artif Organs* 15(6):474–480.
- Tan J, Hytiroglow P, Wieczorek R, Park Y, Thung S, Arias B, Theise N. 2002. Immunohistochemical evidence for hepatic progenitor cells in liver diseases. *Liver* 22:365.
- Theise ND. 2003. Liver stem cells: Prospects for treatment of inherited and acquired liver diseases. *Expert Opin Biol Ther* 3(3):403–408.
- Theise ND, Nimmakayalu M, Gardner R, Illei PB, Morgan G, Teperman L, Henegariu O, Krause DS. 2000. Liver from bone marrow in humans. *Hepatology* 32(1):11–16.
- Tompkins RG, Carter EA, Carlson JD, Yarmush ML. 1988. Enzymatic function of alginate immobilized rat hepatocytes. *Biotechnol Bioeng* 31:11–18.
- Tilles AW, Berthiaume F, Yarmush ML, Tompkins RG, Toner M. 2002a. Bioengineering of liver assist devices. *J Hepatobiliary Pancreat Surg* 9(6):686–696.
- Tilles AW, Berthiaume F, Yarmush ML, Toner M. 2002b. Critical issues in bioartificial liver development. *Technol Health Care* 10(3–4):177–186.
- van de Kerkhove MP, Hoekstra R, Chamuleau RA, van Gulik TM. 2004. Clinical application of bioartificial liver support systems. *Ann Surg* 240(2):216–230.
- Vessey CJ, de la Hall PM. 2001. Hepatic stem cells: A review. *Pathology* 33(2):130–141.
- Viravaidya K, Sin A, Shuler ML. 2004. Development of a microscale cell culture analog to probe naphthalene toxicity. *Biotechnol Prog* 20(1):316–323.
- Xu J, Ma M, Purcell WM. 2003. Characterisation of some cytotoxic endpoints using rat liver and HepG2 spheroids as in vitro models and their application in hepatotoxicity studies. II. Spheroid cell spreading inhibition as a new cytotoxic marker. *Toxicol Appl Pharmacol* 189(2):112–119.
- Yarmush ML, Dunn JC, Tompkins RG. 1992a. Assessment of artificial liver support technology. *Cell Transplant* 1(5):323–341.
- Yarmush ML, Toner M, Dunn JC, Rotem A, Hubel A, Tompkins RG. 1992b. Hepatic tissue engineering. Development of critical technologies. *Ann N Y Acad Sci* 665:238–252.
- Zeilinger K, Holland G, Sauer IM, Efimova E, Kardassis D, Obermayer N, Liu M, Neuhaus P, Gerlach JC. 2004. Time course of primary liver cell reorganization in three-dimensional high-density bioreactors for extra-corporeal liver support: An immunohistochemical and ultrastructural study. *Tissue Eng* 10(7–8):1113–1124.